Equalization with Interference Cancellation for OFDM/OQAM systems

Hao Lin, Pierre Siohan, Philippe Tanguy and Jean-Philippe Javaudin
France Telecom, Orange Labs,
4 rue du Clos Courtel, B.P. 91226
35512 Cesson Sévigné Cedex, France
Email: {hao.lin,pierre.siohan,jeanphilippe.javaudin}@orange-ftgroup.com

***Abstract*— OFDM/OQAM is a multi-carrier modulation scheme that, differently from conventional OFDM, does not require any guard interval. Indeed, the interference that results from a transmission over time and/or frequency selective channels can be partly contained if the pulse shape has been appropriately selected. Nevertheless, for certain transmission conditions, a simple zero-forcing (ZF) equalization is not enough to cancel this interference. In this paper, we propose an Equalization with Interference Cancellation (EIC) to counteract the performance floor that characterizes OFDM/OQAM systems using a simple ZF equalization. The basic principle rests on an accurate computation of the interference term taking into account the channel and the prototype filter coefficients. The simulation results illustrate the efficiency of the EIC method.**

***Index Terms*— OFDM, OFDM/OQAM, equalization**

I. Introduction

Orthogonal Frequency Division Multiplexing (OFDM) is an efficient Multi Carrier Modulation (MCM) to fight against multi-path fading channels. However its robustness to multi-path propagation effects comes from the insertion of a Cyclic Prefix (CP) and is therefore obtained at the price of a reduced spectral efficiency. As furthermore the rectangular OFDM symbols lead to a $sin(x)/x$ frequency spectrum, several alternatives have been researched to find better MCM schemes w.r.t. the frequency and/or time-frequency localization criteria. In OFDM/OQAM each subcarrier is modulated with an Offset Quadrature Amplitude Modulation (OQAM). This principle has been introduced long ago [1], but it is more recently [2] that OFDM/OQAM has been presented as a viable alternative to OFDM. Thus, relaxing the orthogonality condition to the real field permits the introduction of a pulse shaping that can provide a good localization in time and frequency, which is not possible with OFDM.

Actually, one of the reasons to choose MCMs is owing to its simpler equalization, e.g. OFDM equalizer is basically carried out using one-tap Zero-forcing (ZF) or Minimum Mean Square Error criteria, and that can greatly compensate channel effects. Furthermore, the CP prevents the inter-block interference introduced by the channel delay spread. On the other hand, thanks to the good time/frequency localization feature, OFDM/OQAM does not append any CP. Moreover, if the transmission does not require large-order constellations, one-tap linear equalizer is still feasible [3], [4]. However, this condition can hardly be guaranteed in modern digital communications, wherein, it turns out that a one-tap equalization is not enough to avoid a performance floor [5]. Straightforwardly, we tend to expect some advanced channel equalizers.

Among the existing equalization techniques for pulse shaped MCMs, some of them are particularly based on cosine modulated filter banks (CMFB), e.g. B. Farhang-Boroujeny et al. proposed a post-combiner equalizer for CMFB-based transmultiplexer, where equalization happens at each subcarrier and cooperates with its up and down carriers [6]. But its convergence behavior rises an important issue of complexity. Similarly, Alhava and Renfors proposed an Adaptive Sine/Cosine equalization (ASCET) for CMFB-based transmultiplexer which is relatively less complex and takes advantage of fractionally-spaced equalizer [7]. Besides CMFB, Nedic et al. proposed a per-bin decision feedback equalization (DFE) for OFDM/OQAM [8], where the equalizer is composed by a feed-forward filter and a feed-back filter with their coefficients estimated by Least Mean Square algorithm or Recursive Least Square algorithm, but its complexity still remains high. However, none of these presented equalizers take into account the knowledge of the prototype filter's coefficients. In this paper, we present a DFE-liked equalizer called Equalization with Interference Cancellation (EIC) which takes advantage of this knowledge to precisely calculate the interference value so that we can perfectly remove it. The practical implementation will be introduced as well.

The following sections are organized as: In section II, we recall some of the main features of OFDM/OQAM and its links with CMFB. In section III, we give a short overview of our transmission model and the demodulation with one-tap OFDM/OQAM equalization. In section IV, we analyze the interference of OFDM/OQAM systems. In section V, we present our EIC equalizer. In section VI, we compare the performance of conventional OFDM and OFDM/OQAM with and without EIC. For brevity, in the rest of this paper we name OFDM/OQAM as OQAM.

This paper is based on "Equalization with Interference Cancellation for Hermitian Symmetric OFDM/OQAM systems" by H. Lin, C. Lélé and P. Siohan, which appeared in the Proceedings of the IEEE International Symposium on Power Line Communications and Its Applications, 2008 (ISPLC 2008), Jeju Island, Korea, April, 2008.

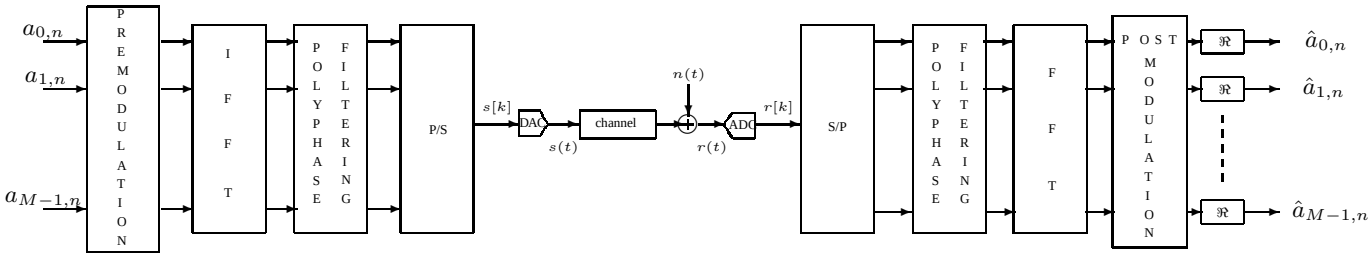

Figure 1. Structure of the transmultiplexer associated to the OFDM/OQAM modulation.

II. Description of OQAM modulation

In this section, we give a short remind of OQAM modulation. The readers who have interests in OQAM can find the details in [2], [9].

A. General description of continuous-time OQAM

The baseband equivalent of a continuous-time OQAM signal can be written as follows [2]:

$$s(t) = \sum_{m=0}^{M-1} \sum_{n \in \mathbf{Z}} a_{m,n} \underbrace{g(t - n\tau_0) e^{j2\pi m F_0 t} e^{j\phi_{m,n}}}_{g_{m,n}(t)}. \quad (1)$$

$$\text{with } \phi_{m,n} = \phi_0 + \frac{\pi}{2}(n+m) \quad (mod \quad \pi), \quad (2)$$

an additional phase term in which ϕ_0 can be arbitrarily chosen, M an even number of sub-carriers, $F_0 = 1/T_0 = 1/2\tau_0$ the subcarrier spacing and g the pulse shape. The transmitted symbols $a_{m,n}$ are real-valued. They are obtained from a 2^{2K}-QAM constellation, taking the real and imaginary parts of these complex-valued symbols of duration $T_0 = 2\tau_0$, with τ_0 the time offset between the two parts [2], [9]–[11].

Assuming a distortion-free channel, perfect reconstruction of real symbols is obtained owing to the following real orthogonality condition:

$$\Re\{\langle g_{m,n} | g_{p,q} \rangle\} = \Re\{\int g_{m,n}(t) g^*_{p,q}(t) dt\} = \delta_{m,p}\delta_{n,q}, \quad (3)$$

where $*$ denotes the complex conjugation, $\delta_{m,p} = 1$ if $m = p$ and $\delta_{m,p} = 0$ if $m \neq p$. For concision purpose, we set $\langle g \rangle^{p,q}_{m,n} = \langle g_{m,n} | g_{p,q} \rangle$, with $\langle g_{m,n} | g_{p,q} \rangle$ a pure imaginary term for $(m,n) \neq (p,q)$.

B. General description of discrete-time OQAM

At a sampling period $T_e = \frac{T_0}{M}$, the discrete-time formulation of the baseband OQAM signal (1) is given by

$$s[k] = \sum_{m=0}^{M-1} \sum_{n \in \mathcal{Z}} a_{m,n} \underbrace{g[k - nN] e^{j\frac{2\pi}{M} m\left(k - \frac{L-1}{2}\right)} e^{j\phi_{m,n}}}_{g_{m,n}[k]} \quad (4)$$

where $N = M/2$ is the discrete-time offset and L is the length of the prototype filter g. This modulated signal can be written using the filter bank formalism. Indeed, it is shown in [9] that after a simple premodulation stage, the data on each sub-carrier are filtered by an exponentially modulated version of the prototype filter $g[k]$. This implementation can be based, as for OFDM, on an Inverse Fast Fourier Transform (IFFT). Similarly, at the receiver side the dual operations are carried out. The overall structure thus corresponds to a modulated transmultiplexer (TMUX) where, assuming that the OQAM prototype filter is of unit energy, the synthesis and analysis filter bank, for $m = 0, ..., M-1$, $k = 0, ..., L-1$, are such that:

$$f_m[k] = g[k] e^{j\frac{2\pi}{M} m\left(k - \frac{L-1-N}{2}\right)}, \quad (5)$$

$$h_m[k] = g[k] e^{j\frac{2\pi}{M} m\left(k - \frac{L-1+N}{2}\right)} = f^*_m[L-1-k], \quad (6)$$

respectively. If, as assumed in the rest of the paper, the prototype filter $g[k]$, is real-valued and symmetrical, then $h_m[k] = f_m[k]$ for all m and k. Note that as OQAM has no CP, the prototype length can be limited to the FFT size, i.e. $L_{min} = M$. The prototype filter $G(z)$ can also be expressed as a function of its polyphase components $E_l(z)$ of order $2N$ [12]:

$$G(z) = \sum_{l=0}^{2N-1} z^{-l} E_l(z^{2N}) \quad \text{with} \quad E_l(z) = \sum_n g[l+2N] z^{-n}$$

In [9], it is shown that, for OQAM, one gets a perfect orthogonality if and only if, for $0 \leq l \leq N-1$:

$$E_l(z) E_l(z^{-1}) + E_{l+N}(z) E_{l+N}(z^{-1}) = \frac{1}{N}, \forall z. \quad (7)$$

In Fig. 1, we depict the main building blocks of this OQAM TMUX. The details of the structure can be found in [9]. When a prototype filter satisfies the orthogonality condition (7), then, for a distortion-free channel, extracting the real part, see $\Re(.)$ in Fig. 1, we perfectly recover the transmitted symbol: $\forall (m,n), \hat{a}_{m,n} = a_{m,n}$. However, in practice, for transmission over a realistic channel, the orthogonality property is lost, leading to Inter Symbol Interference (ISI) and Inter Carrier Interference (ICI).

Note also from (7) that for OQAM we recover a Perfect Reconstruction (PR) condition already known for CMFB [12].

III. Channel model

A. OQAM transmission over multi-path channel

For derivation simplicity, we assume the channel is time-invariant. In [3], it is assumed, as also generally the

case for CP-OFDM, that, using a sufficiently high number of sub-carriers, a flat fading happens at each sub-carrier. Then, the baseband version of the received signal, noise taken apart, can be written as follows:

$$\begin{aligned} y(t) &= (h \otimes s)(t) \\ &= \sum_{n\in\mathbf{Z}} \sum_{m=0}^{M-1} a_{m,n} \int_0^{\Delta} h(\tau) g_{m,n}(t-\tau)\, d\tau \\ &= \sum_{n\in\mathbf{Z}} \sum_{m=0}^{M-1} a_{m,n} e^{j\phi_{m,n}} e^{2j\pi m F_0 t} \\ &\times \int_0^{\Delta} h(\tau) g(t-\tau-n\tau_0) e^{-2j\pi m F_0 \tau} d\tau \\ &= \sum_{n\in\mathbf{Z}} \sum_{m=0}^{M-1} a_{m,n} H_m g_{m,n}(t), \end{aligned} \tag{8}$$

with $\otimes$ the convolution operation, Δ the maximum delay spread and $H_m = \int_0^{\Delta} h(\tau) e^{-2j\pi m F_0 \tau} d\tau$, where h denotes channel impulse response (CIR). The last equality in (8) only holds if the prototype function has relatively low variations in time over the interval $[0, \Delta]$ that is, $g(t-\tau-n\tau_0) \approx g(t-n\tau_0)$ for $\tau \in [0, \Delta]$.

B. Demodulation and Zero Forcing equalization

The demodulation of the received signal at the (m_0, n_0) position, noise taken apart, provides a complex symbol given by $y_{m_0,n_0} = \langle y | g_{m_0,n_0} \rangle$. After computations, we get the following expression:

$$y_{m_0,n_0} = H_{m_0} a_{m_0,n_0} + \sum_{(m,n)\neq(m_0,n_0)} a_{m,n} H_m \langle g \rangle_{m,n}^{m_0,n_0} \tag{9}$$

Then, as shown in [3], with ZF equalization and noise taken into apart, for any demodulated signal of index (m_0, n_0) in the time-frequency plane, the estimated symbol is given by

$$\hat{a}_{m_0,n_0} = a_{m_0,n_0} + \Re\{I_{m_0,n_0}\} \tag{10}$$

where,

$$I_{m_0,n_0} = \sum_{(m,n)\neq(m_0,n_0)} a_{m,n} \frac{H_m}{H_{m_0}} \langle g \rangle_{m,n}^{m_0,n_0} \tag{11}$$

is a complex-valued term. $\Re\{I_{m_0,n_0}\}$ can be interpreted as the residual interference due to the channel spreading, and it will be further analyzed in next section. [3] shows that, if the prototype filter is well localized in time and frequency, we can get: $\Re\{I_{m_0,n_0}\} \approx 0$, leading to reliable estimation of a_{m_0,n_0}. Therefore, we can have an accurate detection of a_{m_0,n_0} as long as we know the channel coefficient H_{m_0} on the receiver side. However, the approximations we use for g and $\Re\{I_{m_0,n_0}\}$ are no longer held when the channel delay spread is long or/and when the constellation order is high. Indeed large constellations, e.g. 16-QAM or beyond, require high Signal-to-Noise Ratio (SNR) and then $\Re\{I_{m_0,n_0}\}$ is not negligible compared to noise.

IV. ICI and ISI analysis

A particular feature of OQAM modulation is the overlapping between successive OQAM block symbols. Indeed, as any OQAM filter bank implementation shows, see e.g. [9], the expansion factor, here given by $N = M/2$, is always less than the prototype filter length ($L_{min} = M$). Then at the transmitter side, some potential interferences have already existed even without the presence of channel effects, and these interferences include ICI and ISI. If we take a look at the time-frequency

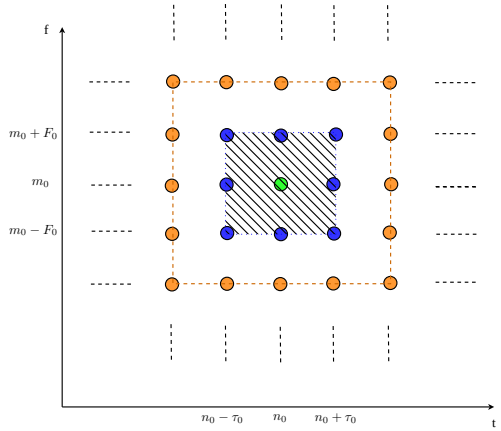

Figure 2. Time-frequency lattice.

lattice of the demodulated OQAM symbols with ideal noiseless channel as shown in Fig. 2, the target symbol a_{m_0,n_0} is interfered by its neighboring symbols. Indeed, the most powerful interferences come from the blue zone symbols where we call them 1-tap neighborhood symbols. Moreover, with increasing the zone size, the power of interferences is decreasing. That is to say if the prototype filter is well localized in time and frequency domain, then the interferences can be limited to a certain zone size, or, certain neighboring taps.

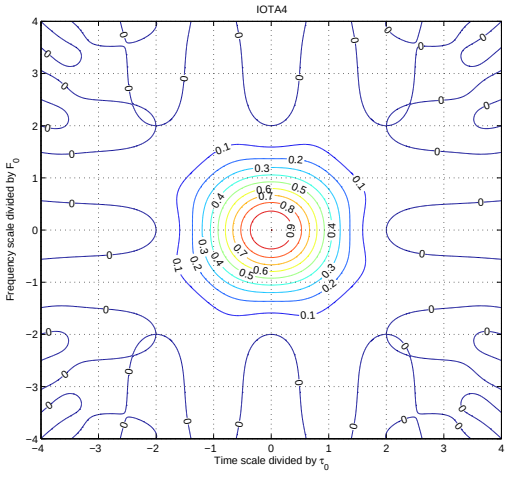

Figure 3. Ambiguity function for the IOTA4 prototype filter.

For example, Fig 3 shows the ambiguity function of a prototype called Isotropic Orthogonal Transform

Algorithm (IOTA) [2], where its energy is isotropically spreading towards the time and frequency. Actually, how far does its energy spread shows how far does one symbol filtered by the prototype filter can impact. Thus, we find that most of the interferences can be limited into a 3-tap neighborhood area. On the other hand, it is worth noting that, although the OQAM modulated signal contains its own interfering components, the demodulation can still re-build the orthogonality. It is because these interferences are pure imaginary valued, which again corresponds to the orthogonal condition (3), i.e. OQAM allows to have non-orthogonality in the imaginary field. Mathematically speaking, let us re-use the demodulation model (9) with distortion-free noiseless channel as

$$\begin{aligned} y_{m_0,n_0} &= a_{m_0,n_0} + \sum_{(m,n)\neq(m_0,n_0)} a_{m,n} \langle g \rangle_{m,n}^{m_0,n_0} \\ &= a_{m_0,n_0} + I_{m_0,n_0}, \end{aligned}$$

where the transmitted symbols a_{m_0,n_0} are real-valued, and as we mentioned before, $\langle g \rangle_{m,n}^{m_0,n_0}$ is pure imaginary valued. Therefore, I_{m_0,n_0} remains pure imaginary valued. Ultimately, that leads to $\Re\{I_{m_0,n_0}\} = 0$. However, in the case of non-ideal channel, $\Re\{I_{m_0,n_0}\} = 0$ is only an approximation and it depends on whether the transmission requires large-order constellations or not. To explain this, we now detail the interference term of (11), which can further be separated into two terms as

$$I_{m_0,n_0} = C_{m_0,n_0} + D_{m_0,n_0}, \tag{12}$$

where

$$C_{m_0,n_0} = \sum_{(p,q)\neq(0,0)} a_{m_0+p,n_0+q} \langle g \rangle_{m_0+p,n_0+q}^{m_0,n_0}, \tag{13}$$

is a pure imaginary term and stands for the interferences that come from the lattice zone where the channel coefficients are assumed to be the same as H_{m_0} (i.e. $H_{m_0+p} = H_{m_0}$). On the other hand,

$$D_{m_0,n_0} = \sum_{(p',q')>(p,q)} a_{m_0+p',n_0+q'} \frac{H_{m_0+p'}}{H_{m_0}} \langle g \rangle_{m_0+p',n_0+q'}^{m_0,n_0} \tag{14}$$

is a complex term and denotes the interferences that come from the lattice zone where the channel is different to H_{m_0} (i.e. $H_{m_0+p'} \neq H_{m_0}$). Then, we can rewrite (10) as

$$\hat{a}_{m_0,n_0} = a_{m_0,n_0} + \Re\{D_{m_0,n_0}\}. \tag{15}$$

It is obvious that D_{m_0,n_0} is independent of noise, which means that increasing SNR can not help to reduce the interference D_{m_0,n_0}. Furthermore, in the large order constellation case, high SNR is always required to obtain a satisfying Bit Error Rate (BER), which corresponds to weak noise. Thus, D_{m_0,n_0} becomes a predominant interference. Thereby, a performance floor appears. However, in the small-order constellation case, these interferences are covered by noise, thus, can be neglected.

V. Two-step Equalization with Interference Cancellation (EIC)

A. Theoretical derivation

In this section, we propose a two-step equalization strategy in order to counteract the performance loss that occurs when the approximations are no longer satisfied, i.e. $g(t-\tau-n\tau_0) \neq g(t-n\tau_0)$ and $\Re\{I_{m_0,n_0}\} \neq 0$.

Then, the demodulated signal at the (m_0, n_0) position, noise taken apart, is given by

$$\begin{aligned} y_{m_0,n_0} &= \langle y | g_{m_0,n_0} \rangle \\ &= \int_{-\infty}^{\infty} \sum_{n\in\mathbf{Z}} \sum_{m=0}^{M-1} a_{m,n} \\ &\times \int_0^{\Delta} h(\tau) g_{m,n}(t-\tau)\, d\tau g_{m_0,n_0}^*(t) dt \\ &= \sum_{n\in\mathbf{Z}} \sum_{m=0}^{M-1} a_{m,n} e^{j(\phi_{m,n}-\phi_{m_0,n_0})} \\ &\times \int_0^{\Delta} h(\tau) e^{-j2\pi m F_0 \tau} f(\tau) d\tau \end{aligned} \tag{16}$$

where,

$$f(\tau) = \int_{-\infty}^{\infty} e^{j2\pi(m-m_0)F_0 t} g(t-\tau-n\tau_0) g^*(t-n_0\tau_0) dt. \tag{17}$$

Substituting in $f(\tau)$ the variables as follows, $t-\tau-n\tau_0 = \mu + \frac{\tau'}{2}$ and $t - n_0\tau_0 = \mu - \frac{\tau'}{2}$, we get

$$\begin{aligned} f(\tau) &= \int_{-\infty}^{\infty} g(\mu + \frac{\tau'}{2}) g^*(\mu - \frac{\tau'}{2}) \\ &\times e^{j2\pi(m-m_0)F_0\left(\mu + \frac{(n_0+n)\tau_0+\tau}{2}\right)} d\mu \\ &= e^{j\pi(m-m_0)F_0((n_0+n)\tau_0+\tau)} \\ &\times A_g[(n_0-n)\tau_0 - \tau, (m-m_0)F_0] \end{aligned} \tag{18}$$

where, $A_g(\tau,\nu)$, the ambiguity function of $g(t)$, is defined as:

$$A_g(\tau,\nu) = \int_{-\infty}^{\infty} g(t+\frac{\tau}{2}) g^*(t-\frac{\tau}{2}) e^{j2\pi\nu t} dt. \tag{19}$$

Substituting (18) into (16) leads to:

$$\begin{aligned} y_{m_0,n_0} &= \sum_{n\in\mathbf{Z}} \sum_{m=0}^{M-1} a_{m,n} e^{j(\phi_{m,n}-\phi_{m_0,n_0})} \\ &\times \int_0^{\Delta} h(\tau) e^{-j2\pi m F_0 \tau} f(\tau) d\tau \\ &= a_{m_0,n_0} \int_0^{\Delta} h(\tau) e^{-j2\pi m_0 F_0 \tau} A_g(-\tau, 0) d\tau + J_{m_0,n_0} \end{aligned}$$

where the complex-valued term J_{m_0,n_0}, summation of ISI and ICI for a given time-frequency point (m_0, n_0), is:

$$\begin{aligned} J_{m_0,n_0} &= \sum_{(m,n)\neq(m_0,n_0)} a_{m,n} e^{j(\phi_{m,n}-\phi_{m_0,n_0})} \\ &\times e^{j\frac{\pi}{2}(m-m_0)(n_0+n)} \int_0^{\Delta} h(\tau) e^{-j\pi(m_0+m)F_0\tau} \\ &\times A_g[(n_0-n)\tau_0 - \tau, (m-m_0)F_0] d\tau. \end{aligned}$$

Based on the two previous equations, an ideal equalization with interference cancellation would provide equalized data symbols given by:

$$\hat{a}_{m_0,n_0} = \Re\left\{ \frac{y_{m_0,n_0} - J_{m_0,n_0}}{\int_0^\Delta h(\tau) e^{-j2\pi m_0 F_0 \tau} A_g(-\tau, 0) d\tau} \right\}.$$

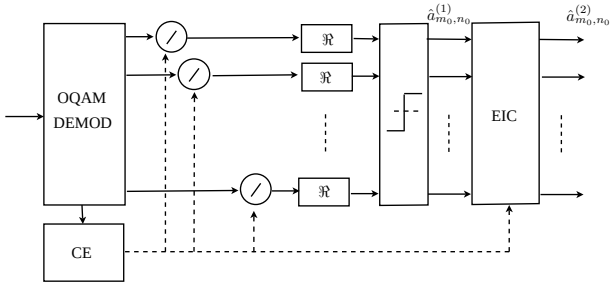

Figure 4. Receiver structure with EIC equalizer.

The receiver structure depicted in Fig. 4 shows a practical implementation of this ideal equalizer. In a first step, we get equalized data symbols such that

$$\hat{a}^{(1)}_{m_0,n_0} = \text{HD}\left[\Re\left\{ \frac{y_{m_0,n_0}}{\hat{H}_{m_0}} \right\} \right], \tag{20}$$

where HD$[\cdot]$ denotes hard decision, $\hat{H}_{m_0}$ stands for the estimated channel coefficient at frequency m_0, which can be obtained using Channel Estimation (CE) [3].

In a second step, we compute the channel time response, $\hat{h}(\tau)$, Inverse Fourier Transform (IFT) of $\hat{H}^{(c)}_m$ with $m = 0, \cdots, M-1$. Thus, we can get an estimated value of the interference term

$$\begin{aligned} \hat{J}_{m_0,n_0} &= \sum_{(m,n)\neq(m_0,n_0)} \hat{a}^{(1)}_{m,n} e^{j(\phi_{m,n} - \phi_{m_0,n_0})} \\ &\times \; e^{j\frac{\pi}{2}(m-m_0)(n_0+n)} \int_0^\Delta \hat{h}(\tau) e^{-j\pi(m_0+m)F_0\tau} \\ &\times \; A_g[(n_0-n)\tau_0 - \tau, (m-m_0)F_0] d\tau. \end{aligned} \tag{21}$$

Finally, using the interference cancellation principle, we find equalized data symbols given by

$$\hat{a}^{(2)}_{m_0,n_0} = \Re\left\{ \frac{y_{m_0,n_0} - \hat{J}_{m_0,n_0}}{\int_0^\Delta \hat{h}(\tau) e^{-j2\pi m_0 F_0 \tau} A_g(-\tau, 0) d\tau} \right\}. \tag{22}$$

B. Implementation algorithm

However, if a direct computation based on (22) implements a nearly-perfect ICI and ISI cancellation, it also requires with (21) a computational complexity of order M^2 for each time-frequency point (m_0, n_0), with M generally being a fairly large number. In practice, this complexity can be reduced taking into account the three following facts.

Firstly, as discussed in section IV, with a time-frequency well-localized prototype filter, the summation in (21) can be limited to a small size neighborhood around (m_0, n_0). Let $\Omega^*_{\Delta m,\Delta n}$ denote this neighborhood with $\Omega^*_{\Delta m,\Delta n} = \Omega_{\Delta m,\Delta n} - (0,0)$ and $\Omega_{\Delta m,\Delta n} = \{(m_0 + p, n_0 + q), |p| \leq \Delta m, |q| \leq \Delta n\}$. The main interference terms are due to the closest positions, i.e. $|p|$ and $|q|$ less or equal 3 for IOTA case.

Secondly, $\hat{J}_{m_0,n_0}$ can be computed with FFTs.

Thirdly, since the channel delay spread Δ is significantly less than T_0 (in discrete time, this means that the channel length, we denote by L_h, is only a fraction of M), then the computation complexity may be further reduced with pruned FFTs.

Let us illustrate more in details this three-step reduction of complexity using, for example, a neighborhood $\Omega^*_{1,1}$, also called 1-tap neighborhood, where $|p| = |q| \leq 1$. Without loss of generality, we assume that the phase term in (2) is such that $\phi_0 = 0$. Then, the interference can be expressed as

$$\begin{aligned} \hat{J}_{m_0,n_0} &= \sum_{(p,q)\in\Omega^*_{1,1}} \hat{a}^{(1)}_{m_0+p,n_0+q} e^{j\frac{\pi}{2}(p+q)} e^{j\frac{\pi}{2}p(2n_0+q)} \\ &\times \; \int_0^\Delta \hat{h}(\tau) e^{-j\pi(2m_0+p)F_0\tau} A_g(-q\tau_0 - \tau, pF_0) d\tau. \end{aligned}$$

As in discrete-time, we have $T_0 = 2\tau_0 = 1/F_0 = MT_e$, the 1-tap neighborhood interference becomes:

$$\hat{J}_{m_0,n_0} = \sum_{(p,q)\in\Omega^*_{1,1}} \hat{a}^{(1)}_{m_0+p,n_0+q} e^{j\frac{\pi}{2}(p+q+pq+2pn_0)} B_{m_0}[q,p], \tag{23}$$

where

$$B_{m_0}[q,p] = \sum_{k=0}^{L_h-1} \hat{h}[k] A_g\left[-q\frac{M}{2} - k, pF_0 \right] e^{-j\frac{\pi(2m_0+p)k}{M}}. \tag{24}$$

Note that in the computation of $B_{m_0}[q,p]$ all terms related to the ambiguity function can be calculated off-line and also that, since $B_{m_0}[q,p]$ does not depend on n_0, it only needs to be evaluated at the preamble rate, i.e. at a slow rate. Furthermore, this computation can be computed by FFTs. First of all, for a given m_0, when $p = 0$, we have:

$$B_{m_0}[q,p=0] = \sum_{k=0}^{L_h-1} \hat{h}[k] A_g\left[-q\frac{M}{2} - k, 0 \right] e^{-j\frac{2\pi m_0 k}{M}},$$

and for $|p| = 1$ we have:

$$B_{m_0}[q,p] = \sum_{k=0}^{L_h-1} \hat{h}[k] A_g\left[-q\frac{M}{2} - k, pF_0 \right] e^{-j\frac{2\pi(2m_0+p)k}{2M}}.$$

As $\hat{h}[k]$ is zero for $k \geq L_h$, both quantities can be obtained as pruned FFTs [13] of size M and $2M$, respectively. For $p = 0$, the vector $\mathbf{B}_m[q,0]$ is calculated by an M-point pruned FFT of $\hat{h}[k] A_g\left[-q\frac{M}{2} - k, 0\right]$. For $p = 1$, $\mathbf{B}_m[q,p]$ corresponds to the even polyphase components of a $2M$-point pruned FFT of $\hat{h}[k] A_g\left[-q\frac{M}{2} - k, pF_0\right]$. Then, using the symmetry property of the ambiguity function $A_g(\tau,\nu)$, (i.e. $A_g(\tau,\nu) = A_g(\tau,-\nu)$), $\mathbf{B}_m[q,-p]$ does not need to be calculated again, and it is only a frequency shift version of $\mathbf{B}_m[q,p]$. Moreover, for $q = p = 0$, an M-point pruned FFT of $\hat{h}[k] A_g[-k, 0]$ gives the denominator coefficients of (22).

Consequently, the overall computational cost of the interference calculation is in $O(M \log_2 L_h)$. A more general complexity analysis as a function of the neighboring taps will be shown later.

VI. Simulation results

In our simulations, we compare CP-OFDM with OQAM with/without EIC over a multi-path channel model with constellation orders from small to large. Moreover, we first consider the case of a transmission without channel coding, then the simulation results with channel coding will be shown to check the efficiency of EIC equalizer.

A. Simulation parameters and channel model

The main parameters of the transmission system are:

- Sampling frequency: 10 MHz;
- Constellation: 4, 16, 64-QAM;
- FFT size: 128;
- CP length: maximum channel delay spread plus 2 samples ($L_h + 2$);

The simulations are carried out with discrete-time models and prototype filters of finite length that are all optimized w.r.t. the time-frequency localization (TFL). Thus, the IOTA prototype function [2] used is truncated, and has a duration of $4T_0$ leading to a length $L = 4M = 512$. It is designated as IOTA4.

Note that since the objective of our simulations is to evaluate EIC performance, we assume perfect channel estimation at the receiver i.e. the receiver knows perfectly channel coefficients. The channel model, in our simulations, is a simple 2-path Rayleigh channel with Line-of-Sight (LOS) propagation. The complex coefficients of the two paths, named α_1 and α_2, are independently generated and with power profiles (in dB): $-4, -15$, i.e. $E\{|\alpha_1|^2\} = 0.398$ and $E\{|\alpha_2|^2\} = 0.03162$. Moreover, in order to guarantee the LOS propagation, we set the amplitude of α_1 to be at least 4 dB stronger than that of α_2 in each channel realization. The channel coefficients are normalized before being applied to simulations, such that, the normalized coefficients of the two paths are $\alpha_1' = \frac{\alpha_1}{\sqrt{\sum_n E\{|\alpha_n|^2\}}}$ and $\alpha_2' = \frac{\alpha_2}{\sqrt{\sum_n E\{|\alpha_n|^2\}}}$, with $n = 1, 2$. Furthermore, since OQAM modulation is pretty sensitive to the delay spread, therefore, the delay profile of this model is set to around 12.5% of FFT interval (1.6 μs) and 16.7% of FFT interval (2.31 μs), respectively. Note also that we assume that the channel remains non-variant during 20 symbols duration (0.288 ms).

B. Simulation results

The simulation results, in BER versus SNR, expressed as E_b/N_0, are depicted in Figs. 5, 6, 7 for 4, 16 and 64-QAM, respectively. Each figure has 4 curves which are CP-OFDM with CP length of $L_h + 2$ where $L_h = \frac{M}{8}$ (1.6 μs), OQAM with simple one-tap ZF, OQAM with EIC and ideal OFDM, where ideal OFDM corresponds to CP-OFDM without considering the loss due to CP.

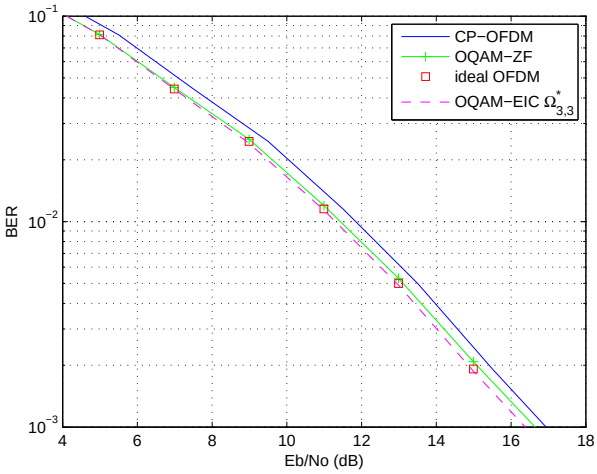

Figure 5. BER versus E_b/N_0 for uncoded 4-QAM with $L_h = \frac{M}{8}$.

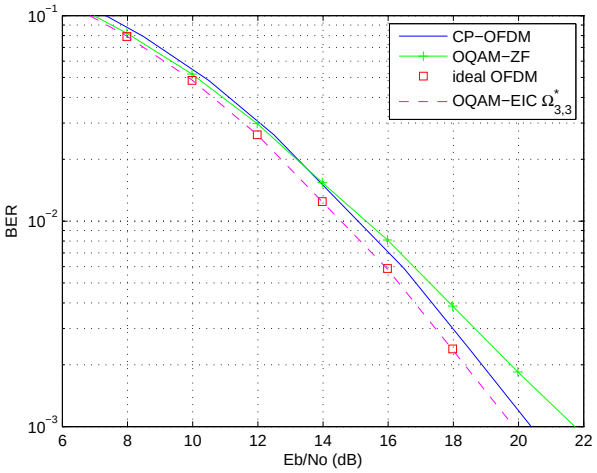

Figure 6. BER versus E_b/N_0 for uncoded 16-QAM $L_h = \frac{M}{8}$.

For 4-QAM in Fig. 5, let us first see the difference between CP-OFDM versus ideal OFDM. Since the CP length of OFDM is longer than the maximum channel delay spread, then we can expect an ICI/ISI-free transmission. That is to say the performance decay of CP-OFDM, compared to the ideal OFDM bound, is due to the loss of spectral efficiency, which can be calculated by $10 \log_{10} \frac{128+18}{128} \approx 0.57$ dB. Next we take a look at the case of OQAM with ZF versus CP-OFDM. Since OQAM does not apply CP, then it fully gains spectral efficiency, but compared to ideal OFDM, OQAM still has a performance loss which reveals one-tap ZF can not perfectly cancel interference. Besides, the performance floor problem of OQAM with ZF is not that obvious in 4-QAM case, that proves what we mentioned before: when noise is more powerful than interference, ZF equalizer remains feasible for OQAM system. On the other hand, the curve of OQAM with EIC is totally superposed with that of ideal OFDM, which proves that the EIC equalizer can perfectly cancel the interference.

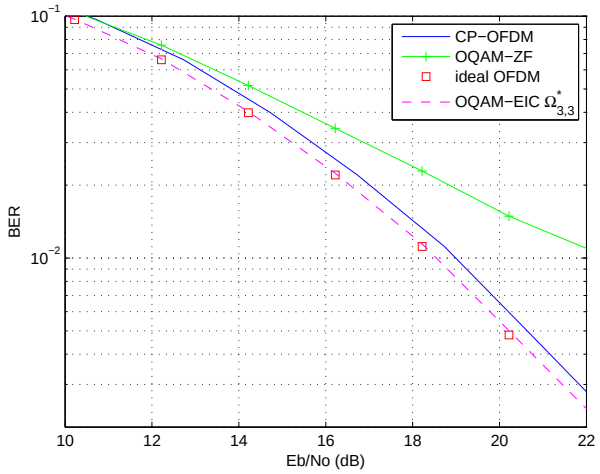

Figure 7. BER versus E_b/N_0 for uncoded 64-QAM $L_h = \frac{M}{8}$.

Fig. 6, 7 show that when increasing the constellation order, the results are relatively changing. The first insight points to OQAM with ZF where a performance floor problem appears in a more obvious way. This again proves that, when constellation order gets larger, the system requires more SNR for satisfactory transmission. In this case, the remaining interference of OQAM turns to be a serious issue that one-tap ZF equalizer is no longer be able to fix. Differently, in OQAM with EIC case, its performance curve always attaches the one of ideal OFDM even with 64-QAM constellation.

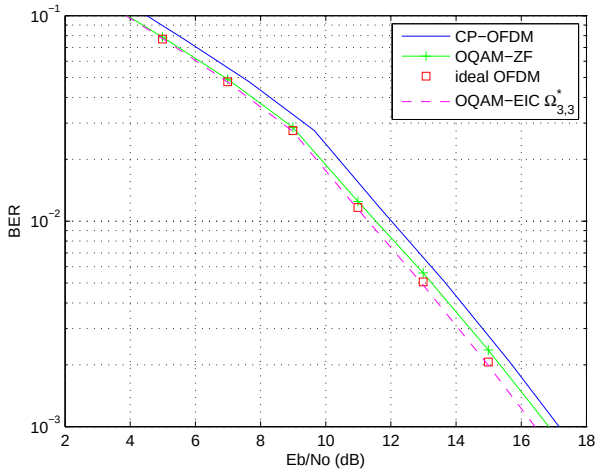

Figure 8. BER versus E_b/N_0 for uncoded 4-QAM $L_h = \frac{M}{6}$.

Next, since OQAM system is fairly sensitive to channel delay spread, thereby, we enlarge the channel delay spread length to evaluate how far can EIC equalizer go. This time we set our channel delay spread to $L_h = \frac{M}{6}$ $(2.31\ \mu s)$. In the cases of 4, 16-QAM as shown in Fig. 8, 9, EIC can have the same performance as ideal OFDM. Moreover, compared to CP-OFDM, the spectral gain increases to $10\log_{10}\frac{128+23.34}{128} \approx 0.73$ dB. Thus, we can say that until now EIC equalizer performs perfectly on interference cancellation. Although, for the last case of 64-QAM in Fig. 10, the curve of OQAM with EIC tends to intersect with that of CP-OFDM, however, we can reasonably expect that channel coding can help to compensate this performance delay.

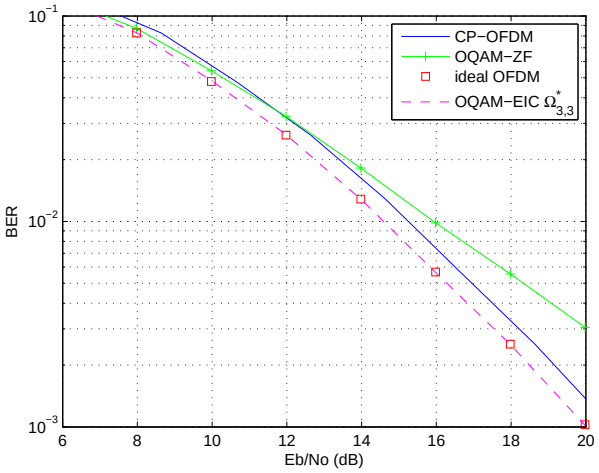

Figure 9. BER versus E_b/N_0 for uncoded 16-QAM $L_h = \frac{M}{6}$.

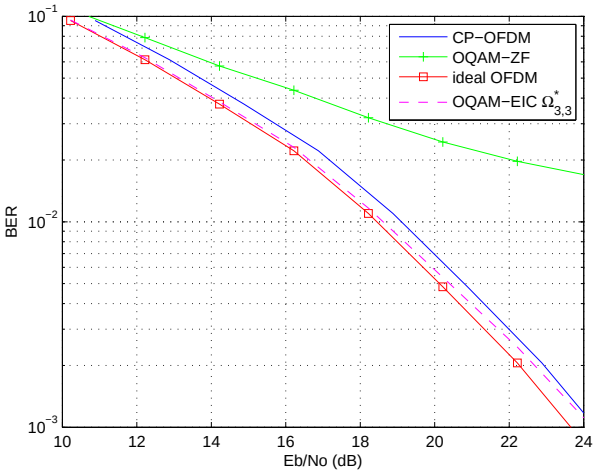

Figure 10. BER versus E_b/N_0 for uncoded 64-QAM $L_h = \frac{M}{6}$.

Finally, we re-simulate the worst case for OQAM: 64-QAM, $L_h = \frac{M}{6}$, and this time we use convolutional channel coding ($R = \frac{1}{2}$, $K = 7$, $g_0 = 133_{\text{oct}}$, $g_1 = 171_{\text{oct}}$). The performances are depicted in Fig. 11, the curve of OQAM with EIC returns back to the expected place. Conservatively speaking, for this simulation model, EIC equalizer with convolutional coding can perfectly cancel interference and retain the spectral efficiency gain with constellation up to 64-QAM, as long as the maximum channel delay spread is less than 16.7% of FFT interval.

C. Complexity evaluation

Speaking of the complexity, OQAM with EIC has two types of computation. One is the calculations that are

TABLE I.
COMPUTATIONAL COMPLEXITY OF κ-TAP NEIGHBORHOOD EIC EQUALIZER: FFT SIZE M, CHANNEL LENGTH L_h.

	M_r	A_r	D_r
off-line	$(8\kappa^2+8\kappa+4)M\log_2 L_h - 4L_h$	$(4\kappa^2+4\kappa+2)(3M\log_2 L_h + 2M) - (2\kappa^2+3\kappa+3)2L_h$	0
on-line	$(16\kappa^2+16\kappa+6)M$	$(16\kappa^2+16\kappa)M$	$2M$

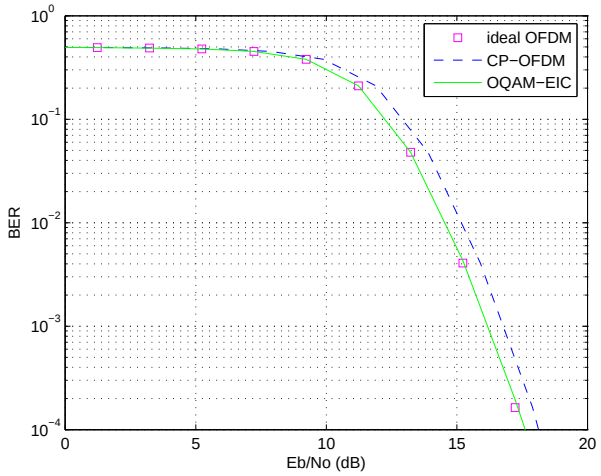

Figure 11. BER versus E_b/N_0 for 64-QAM with convolutional code and $L_h = \frac{M}{6}$.

triggered only once when the estimated channel coefficients are updated. Furthermore, the calculation can be implemented off-line. Thus, we denote this type as off-line computation. The other one is the calculations that need to be carried out in each τ_0 symbol period, we denote this one as on-line computation. The extra computations of EIC are: the off-line computations of calculating the estimated CIR by an IFFT and a calculation of a part of $\hat{J}_{m_0,n_0}$ i.e., $B_{m_0}[q,p]$ in (24). Plus, the on-line computations of calculating the rest part of $\hat{J}_{m_0,n_0}$ (23); a subtraction $(y_{m_0,n_0} - \hat{J}_{m_0,n_0})$ in (22) and a vector division of (22). Numerically, Markel's algorithm shows that a pruning output sample with length-L of M-point FFT [14] (i.e. assuming that only the first L, $L < M$, output points are needed) requires $2M\log_2 L - 4L$ real multiplications (M_r), and $3M\log_2 L + 2M - 4L$ real additions (A_r). While, Skinner's algorithm shows that a pruning input sample with length-L of M-point FFT [15] requires $2M\log_2 L$ (M_r), and $3M\log_2 L + 2M - 2L$ (A_r). Thus, with reference to the symmetry property of ambiguity function in section. V-B, we layout the computational complexity of EIC equalizer with $\Omega^*_{\kappa,\kappa}$ in Table I, assuming that one complex multiplication needs 4 M_r and 2 A_r; one complex addition needs 2 A_r; one complex inversion needs 2 M_r, 1 A_r and 2 real division (D_r).

VII. CONCLUSION

In this paper, we have presented an equalization algorithm, named Equalization with Interference Cancellation (EIC), that counteracts the error floor effect which is characteristic of OFDM/OQAM modulation schemes with one tap equalization. The efficiency of this method has been illustrated with various simulation results.

REFERENCES

[1] R. W. Chang, "Synthesis of band-limited orthogonal signals for multi-channel data transmission," *Bell. Syst. Tech. Journal*, vol. 45, pp. 1775–1796, Dec. 1966.

[2] B. LeFloch, M. Alard, and C. Berrou, "Coded Orthogonal Frequency Division Multiplex," *Proceedings of the IEEE*, vol. 83, pp. 982–996, June 1995.

[3] C. Lélé, P. Siohan, R. Legouable, and J.-P. Javaudin, "Preamble-based channel estimation techniques for OFDM/OQAM over the powerline," in *ISPLC 2007*, 2007, pp. 59–64.

[4] H. Lin, C. Lélé, and P. Siohan, "Equalization with Interference Cancellation for Hermitian Symmetric OFDM/OQAM systems," in *ISPLC 2008*, April 2008, pp. 363–368.

[5] A. Assalini, M. Trivellato, and S. Pupolin, "Performance Analysis of OFDM-OQAM Systems," in *WPMC '05*, September 2005.

[6] B. Farhang-Boroujeny and L. Lin, "Analysis of Post-Combiner Equalizers in Cosine-Modulated Filterbank-Based Transmultiplexers Systems," *IEEE Transactions on Signal Processing*, vol. 51, no. 12, pp. 3249–3262, Dec. 2003.

[7] J. Alhava and M. Renfors, "Adaptive sine-modulated/cosine-modulated filter bank equalizer for transmultiplexers," in *ECCTD*, Aug 2001, pp. 337–340.

[8] S. Nedic and N. Popovic, "Per-bin DFE for Advanced OQAM-based Multicarrier Wireless Data Transmission Systems," in *2002 international Zurich Seminar on Broadband Communications Access-Transmission-Networking*, Feb 2002, pp. 38–1–6.

[9] P. Siohan, C. Siclet, and N. Lacaille, "Analysis and design of OFDM/OQAM systems based on filterbank theory," *IEEE Transactions on Signal Processing*, vol. 50, no. 5, pp. 1170–1183, May 2002.

[10] B. Hirosaki, "An orthogonally multiplexed QAM system using the discrete Fourier transform," *IEEE Trans. on Communications*, vol. 29, no. 7, pp. 982–989, July 1981.

[11] H. Bölcskei, "Orthogonal frequency division multiplexing based on offset QAM," in *Advances in Gabor Analysis*. Birkhäuser, 2003.

[12] P. P. Vaidyanathan, *Multirate systems and filter banks*. Englewood Cliffs, New-York, New Jersey: Prentice Hall, 1993.

[13] H. V. Sorensen and C. S. Burrus, "Efficient computation of the DFT with only a subset of input or output points," *IEEE Transactions on Signal Processing*, vol. 41, no. 3, pp. 1184–2000, Mar. 1993.

[14] J. D. Markel, "FFT Pruning," *IEEE Trans. Audio Electroacoust*, vol. AU-19, pp. 305–311, Dec. 1971.

[15] D. P. Skinner, "Pruning the decimation-in-time FFT algorithm," *IEEE Tans. Acoust., Speech, SignalProcessing*, vol. ASSP-24, pp. 193–194, Apr. 1976.

Hao Lin received B.S. degree in electrical engineering from Shanghai University, Shanghai, People's Republic of China (PRC), in 2004, and his M.S. degree in mobile communications from Ecole Nationale Supérieure des Télécommunications (ENST) Paris/Eurecom, Sophia Antipolis, France, in 2006, respectively. He is currently a Ph.D. candidate at France Telecom, Orange Labs, Rennes, France. His research interests include Multirate modulations, Signal processing.

Pierre Siohan received the PhD degree from the Ecole Nationale Supérieure des Télécommunications (ENST), Paris, France, in 1989. In 1977 he joined the Centre Commun d'Etudes de Télédiffusion et Télécommunications (CCETT), Rennes, where his activities were first concerned with the communication theory and its application to the design of broadcasting systems. Between 1984 and 1997, he was in charge of the Mathematical and Signal Processing Group. Since September 1997, he has been an Expert Member in the R&D division of France Télécom working in the Broadband Wireless Access Laboratory. His current research interests are in the areas of filter bank design for communication systems and joint source-channel coding.

Philippe Tanguy received the Master degree of research from Université of Rennes 1 in 2008. Since October 2008, he is preparing a PhD in INSA in Rennes, France.

Jean-Philippe Javaudin received an eng. degree from the Ecole Nationale Supérieure des Télécommunications (ENST) in 2001. Since then, he has been working as research engineer at France Telecom R&D in Rennes, France. His main topic of interest is multi-carrier modulation: conventional OFDM and also pulse-shaped OFDM (e.g. IOTA-OFDM). From 2004 to 2007 he contributed to the WINNER FP6 project. Since January 2008 Jean-Philippe Javaudin is the Coordinator of the OMEGA ICT FP7 project.